CONTINUOUS DAMAGE MECHANICS MODEL OF FRACTURE IN LAMINATED COMPOSITES

M. P. Wnuk* and R. D. Kriz

National Bureau of Standards, Boulder, CO 80303, USA

ABSTRACT

A modified version of the Kachanov damage accumulation law is employed to study the damage kinetics in laminated composite materials, such as epoxy/graphite laminates embrittled by low (76K) temperatures.

KEYWORDS

Composites; expoxy/graphite; mechanical properties; damage accumulation; fracture.

INTRODUCTION

Changes in the inner structure of multiphase materials leading to the failure of a structural component can be divided into two basic stages. The first one includes formation and growth of microscopic damages such as vacancies, voids, micropores, and the like, randomly distributed throughout the body. This stage can be called a "latent" phase of fracture process. It is terminated at the instant when the micro-defects localize in a small volume of material leading to a formation of a dominant macroscopic crack. Propagation of this "visible crack" constitutes the second stage of fracture process. When the length of such a crack or its rate reaches the critical value, the final rupture of a component takes place.

MATHEMATICAL MODELING OF DAMAGE ACCUMULATION

Now, we shall focus attention on the failure process which begins with the appearance of the characteristic damage state and ends with the total loss of structural integrity of the composite laminate.

---

*On leave from the University of Wisconsin--Milwaukee

Although the primary component of the damage in this stage is the fiber breaks, which are generated ahead of the dominant crack shown in Fig. 1a, it is realized that other forms of damage, such as matrix cracking, void growth and coalescence, are also present. The theory which allows one to model the process of damage accumulation and the associated extension of the dominant crack which interacts with the damage field stems from the continuous damage mechanics (CDM). This model accounts for stress redistribution due to advancement of the crack and allows one to describe the effect of such stress redistribution on the rate of damage growth. The basic assumption underlying the mathematical modeling involved in the present work is the modified version of Kachanov's law (1966). In its original form the Kachanov law relates the rate of damage growth $d\omega/dt$ to the net section stress, s, i.e.,

$$d\omega/dt = Cs^{\nu} \tag{1}$$

Here C and ν are material constants, while the net section stress s ($= P/A_{eff}$) and the nominal stress σ ($= P/A_o$) are related as follows

$$s = \frac{P}{A_{eff}} = \frac{P}{A_o(1-\omega)} = \frac{\sigma}{1-\omega} \tag{2}$$

The scalar quantity ω, which has been identified as the internal damage parameter, represents the deterioration of the cross-section which transmits the tensile load due to the formation and accumulation of microdefects. If the area actually transmitting the load is called the "effective area," A_{eff}, then ωA_o represents the fraction of the initial area A_o which no longer transmits any load. An example of a law of damage accumulation is the Kachanov equation, which in its classic form may be obtained by combining equations (1) and (2) as follows:

$$\frac{d\omega}{dt} = C\left(\frac{\sigma}{1-\omega}\right)^{\nu} \tag{3}$$

This equation defines the time-dependent quantity ω as a function of the uniform stress σ. A modified version of the basic equation (3) reads

$$\frac{d\omega}{dt} = C\left(\frac{\sigma_\Sigma}{1-\omega}\right)^{\nu} \tag{4}$$

in which the stress σ_Σ no longer is the uniform tensile stress but equals the actual stress occurring at the front of an initial stress concentrator such as a sharp crack. Although equation (4) may be readily integrated

$$\omega(r,t) = 1 - \left[1-C(\nu+1)\int_0^t \sigma_\Sigma^{\nu}\,[r(\tau),\tau]\,d\tau\right]^{\frac{1}{\nu+1}} \tag{5}$$

this form is not of much help unless one provides further details concerning the stress σ_Σ generated (a) ahead of the stationary crack for the latent phase of the fracture process, and (b) ahead of a moving crack for the second phase of the fracture process.

If time is eliminated consistently whenever it appears in the problem, equation (5) may be expressed in the following form:

$$\frac{da}{dt} = \frac{-C\,\sigma_\Sigma^{\nu}(a)}{C\int_{a_o}^{a}\frac{\partial}{\partial a}\sigma_\Sigma^{\nu}(a,a')\frac{da'}{\dot{a}'} + \frac{d\Omega_1(a,a_o)}{da}} \tag{6}$$

Here the symbol $\dot{a}'$ denotes the rate of crack growth evaluated at the instant t', or, equivalently, for the crack length a'. We note that $\dot{a}'$ is a shorthand notation for $\dot{a} = \dot{a}(a')$. Both terms appearing in the denominator of equation (6) involve not only stress σ_Σ but also its gradient $d\sigma_\Sigma/dr$ (or $d\sigma_\Sigma/da$, since "a" is used as a yardstick to measure the current distance from the crack tip). The only quantity yet unexplained is $\Omega_1(a, a_o)$. Ω_1 is the amount of damage generated at the point P (see Figs. 1b and 2) at the end of the latent phase of fracture ($t = t_1$). During this phase, the crack remains stationary, and its length equals a_o. In general, the damage parameter Ω is defined by the following equation:

$$\Omega = \int_0^{\omega}(1-\omega')^{\nu}d\omega' = \frac{1-(1-\omega)^{\nu+1}}{\nu+1} \tag{7}$$

It is seen that the lower limit for Ω is zero (corresponding to the undamaged state, $\omega = 0$), while the upper limit of Ω (corresponding to the "saturation" level of damage, $\omega = 1$), is the critical value $\Omega_c = (1+\nu)^{-1}$. The damage parameter Ω is directly related to stress σ_Σ, that is

$$\Omega(r,t) = C\int_0^t \sigma_\Sigma^{\nu}\,[r(\tau),\tau]\,d\tau \tag{8}$$

In fact, equation (8) may be used to formulate the fracture criterion based on the damage accumulation concept. The criterion may be verbalized as follows: for a collapse of a material element located at the distance r from a dominant crack tip, (which generates the stress field $\sigma_\Sigma(r,t)$), it is necessary that the time integral of ν-th power of the stress at that point, σ_Σ, attains the critical value, Ω_c.

To evaluate the amount of damage generated at any instant during the latent phase of the fracture process ($0 \le t \le t_1$), say Ω'_1, we substitute $\sigma_\Sigma(a, a_o)$ for σ_Σ in equation (8). Plots of Ω'_1 vs. the reduced distance from the crack tip, $r_o/\rho_* = \xi_o$, obtained at two values of the normalized time t/t_1 are shown in Fig. 3a. These plots were constructed assuming certain input data for $Y(r_o)/Y_*$, i.e., the stress distribution ahead of the dominant ply-crack shown in Fig. 1a. An analytical form of the function $Y(r_o)$ was obtained by a Hermitian interpolation performed on the numerical solution by the finite element method, Kriz (1982).

The distinct differences between the distributions of damage shown in Fig. 3b suggest that the exponent ν has a very strong effect on the nature of the damage accumulation process. For $\nu > 1$ there is only a minimal amount of damage generated during the latent stage of fracture at a site some distance away from the crack front. However, the opposite is true for $\nu < 1$, e.g., $\nu = 0.1$ When $\nu << 1$, the damage built up at the control point P during the time interval $(0, t_1)$ nearly reaches the critical level. Upon completion of the latent phase relatively little life is left for the material element located at P. Therefore, the propagation phase rapidly leads to the final rupture or "sudden death" of the component.

To conclude this section let us evaluate the "residual damage", Ω_2, which is the amount of damage generated at a given point while the crack front is advancing toward that point. Evaluation of Ω_2 involves numerical integration of the expression

$$\Omega_2 = \left(\frac{\Omega_c}{t_1}\right) \int_{a_o}^{a} \left[\frac{K_I(a')}{K_I(a_o)}\right]^{\nu} \left[\frac{Y(r')}{Y(\rho_*)}\right]^{\nu} \frac{da'}{\dot{a}(a')}, \qquad r' = \rho_* + a - a' \tag{9}$$

in which $\dot{a}(a')$ is found from the equation of a moving crack, i.e., equation (6). Examples of the damage distributions resulting from numerical evaluation of the expression (9) are shown in Fig. 4. Again, to illustrate the distinct differences in possible scenarios of the damage accumulation process, these two values for the Kachanov exponent were used: $\nu = 0.1$ and $\nu = 2$. Since for $\nu < 1$ most of the microstructural damage is generated during the latent stage of fracture, it becomes obvious why in this case the second phase of failure process, i.e., crack propagation, constitutes only a minor part of the total life of the component. The opposite is true for $\nu > 1$. This effect is demonstrated by the three curves shown in Fig. 5a which represent the final outcome of the mathematical model, namely the integral curves resulting from a numerical solution of the integro-differential equation (6). Note that both the crack length and time, as plotted in Fig. 5a, are nondimensional.

Figure 5b shows the three curves representing the three hypothetical failure processes obtained for $\nu = 2$, the characteristic structural length $\rho_*/b = .02$ and the initial crack length $x_o = a_o/\rho_* = 10$, for the three different states of stress generated ahead of the dominant ply crack. The trend in the failure development process, shown in Fig. 5b, is the same as that inferred from the stress analysis by the finite element method performed by Kriz (1982) for the cracked epoxy/graphite laminates exposed to low temperature (76K).

DISCUSSION OF RESULTS AND CONCLUSIONS

Although the stacking sequence of the laminate used in Kriz's experiment $[0, 90°, +45°, -45°]_S$, differs from the stacking sequence $[90°, 0°]_S$ for which our calculations have been performed, the basic conclusions of this work may be extended to other geometries; and, in particular, they remain valid for the laminates with the stacking sequences favoring formation of the transverse matrix cracks (1978, 1982a) during the early stages

of damage accumulation process. Figure 6 shows an edge view of a specimen which would exactly correspond to the geometrical configuration of a double edge-notch tensile specimen chosen for the numerical examples presented in the preceding sections.

Figure 7 shows an example of the Ω_2 evaluated at $\nu = 0.1$ from the exact equation (14) and from the approximate equation (18). The conclusion is that the approximate form (18) provides a valuable tool for an evaluation of the damage generated during the propagation phase whenever the Kachanov exponent ν is small relative to one. Moreover, the numerical tests have shown that when $\nu << 1$, the value of Ω_2 obtained for any pair of numbers x_o and x becomes negligibly small as compared to the value of Ω_1 evaluated at $t = t_1$, namely

$$\Omega_1 = \Omega_c \left[Y(r_o)/Y(\rho_*)\right]^{\nu} \tag{10}$$

This equation along with the expression defining the incubation time, t_1

$$\left[\int_o^{t_1} \sigma^{\nu}(t)dt\right]_{\nu << 1} = \lim_{\nu \to o} \left\{\frac{\Omega_c}{C} \frac{(2\pi\rho_*)^{\nu/2}}{K_I^{\nu}(a_o)Y_*^{\nu}}\right\} \tag{11}$$

provides the basis for quantifying the two phases of the failure process in laminated composites. The first and the second critical times can now be estimated using these relationships. When the "time zero" is identified with the establishment of the critical damage state (CDS), and when it may be shown that the Kachanov exponent ν does indeed assume values close to zero, then we obtain the following estimates ($\sigma << \sigma_c$):

$$t_1 \simeq (\Omega_c/\sigma_c^{\nu}C)(2\rho_*/a_o)^{\nu/2}/F^{\nu}(a_o/b)Y_*^{\nu}$$

$$\Omega_1 = \Omega_c[Y(r_o)/Y(\rho_*)]^{\nu}, \; r_o = \rho_* + a - a_o \tag{12}$$

(in which σ_c denotes the ultimate tensile strength of the reinforcing fiber). Since $\Omega_2 << \Omega_1$, we also have

$$t_2 << t_1 \text{ and } T \simeq t_1 \tag{13}$$

The symbol T denotes the life of the composite laminate and is obtained as the sum of the critical times, $T = t_1 + t_2$. For a general loading history and when the condition $\sigma << \sigma_c$ is not satisfied, the first critical time t_1 has to be evaluated numerically as a root of equation (11). However, when the applied stress is maintained constant upon creation of the characteristic damage state, say $\sigma = \sigma_o = \text{const.}$, and when the LEFM formulae for a pair of edge cracks penetrating a tensile specimen (cf. Fig. 6) are employed, an estimate for the first critical

time results from equation (12). With a constant stress σ_o and $Y_* \simeq 1$, we have

$$t_1 = \frac{\Omega_c}{C\sigma_o^\nu} \left(\frac{2\rho_*}{a_o}\right)^{\nu/2} F^{-\nu}\left(\frac{a_o}{b}\right) \tag{14}$$

The symbol ρ_* denotes here the radius of a reinforcing fiber, a_o is the depth of ply crack, while 2b denotes the width of a component (cf. Fig. 6). The material constants C, Ω_c and ν, which appear in the damage accumulation law (4), must be determined empirically. The function $F = K_I/\sqrt{\rho a_o}$ may be obtained from the LEFM catalog of the K-factors. An alternative way of writing equation (14) is

$$(\sigma_o/\sigma_c)^\nu = B(t_R/t_1) \tag{15}$$

in which the constant B and the reference time t_R are defined as follows:

$$B = \Omega_c \left(\frac{2\rho_*}{a_o}\right)^{\nu/2} / F^\nu \left(\frac{a_o}{b}\right) Y_*^\nu$$

$$t_R = 1/C\sigma_c^\nu \tag{16}$$

Interestingly, equation (15) predicts an experimentally confirmed linear relationship between the logarithm of the nondimensional applied stress, σ_o/σ_c, and the logarithm of the nondimensional time, t_1/t_R, see Fig. 8. The slope of this line is the negative of the reciprocal of the damage exponent ν. Of course, for arbitrary loading histories $\sigma(t)$ it is to be expected that some deviations from the straight line shown in Fig. 8 will occur. Since the slope of this line depends on the Kachanov parameters C and ν, which are inherent in the mathematical model, further research should focus on experimental determination of the load vs. time-to-failure relationship.

ACKNOWLEDGMENTS

This study was sponsored by The Fracture and Deformation Division of the National Bureau of Standards while Professor Wnuk was on leave from the University of Wisconsin--Milwaukee. A portion of the study at low temperatures was sponsored by the Department of Energy, Office of Fusion Energy.

REFERENCES

Rao, C. V. S. K. (1983). A Note on Fracture Toughness of Multiphase Materials, Engng. Fracture Mechanics, 18, 35-38.

Chou, P. C., and R. Croman (1978). Residual Strength in Fatigue Based on the Strength-Life Equal Rank Assumption, J. Comp. Materials, 2, 75-84.

Cook, J., and J. E. Gordon (1964). A Mechanism for the Control of Crack Propagation in a Brittle System, Proc. Royal Soc., A, 282, 508.

Datta, S. K., H. M. Ledbetter, and R. D. Kriz (1982). Calculated Elastic Constants of Composites Containing Anisotropic Fibers. Int. J. Solids Structures, in press.

Hadley, K. (1975). Dilatancy: Further Studies in Crystalline Rock. Ph.D. Thesis, M.I.T., Cambridge, Mass. 1975.

Kachanov, L. M. (1966). Theory of Creep, in Russian, published by Nauka Publishers, Moscow, 1966, also "Some Problems of Creep Fracture Theory," in Advances in Creep Design, Applied Science Publishers, London, 1971, 21-29.

Kriz, R. D. (1982). Influence of Ply Cracks on Fracture Strength of Graphite/Epoxy Laminates at 76K. Effects of Defects in Composite Materials, ASTM STP 836, in press.

Masters, J. E., and K. L. Reifsnider (1982). An Investigation of Cumulative Damage Development in Quasi-Isotropic Graphite/Epoxy Laminates. ibid., 40-62.

Morozov, E. M., and Y. B. Fridman (1966). Crack Analysis as a Method to Study Fracture Characteristics, Zavodskaya Laboratory, No. 8, 977-984, (in Russian), reviewed by M. P. Wnuk (1968) "Review of Some Russian Papers Pertinent to the Fracture of Solids," Techn. Rep. GALCIT SM 67-9, California Institute of Technology, September 1967, also in the book by V. Z. Parton and E. M. Morozov, "Elastic Plastic Fracture Mechanics" (74), translated from Russian, Mir Publishers, Moscow 1978.

Mroz, Z. (1981). Discussion on Session 7. ibid., 405-409.

Reifsnider, K. L., E. G. Henneke, W. W. Stinchcomb, and J. C. Duke (1982a). Damage Mechanics and NDE of Composite Laminates, in Mechanics of Composite Materials: Recent Advances, ed., Z. Hashin and C. T. Herakovich, 399-420.

Reifsnider, K. L. (1982b). Damage in Composite Materials, ASTM STP 775, 552-563.

Rousselier (1981). Finite Deformation Constitutive Relations and Ductile Fracture. Proceedings of IUTAM Symposium on 3D Constitutive Relations and Ductile Fracture. Ed. S. Nemat Nasser, North Holland Publishing Co., 331-355.

Tada, H., P. C. Paris, and G. R. Irwin (1973). The Stress Analysis of Cracks Handbook. Del Research Corp., Hellertown, PA, 1973.

Watt, J. P., G. F. Davies, and R. J. O'Connell (1976). The Elastic Properties of Composite Materials, Reviews of Geophysics and Space Physics. 14, 541-563.

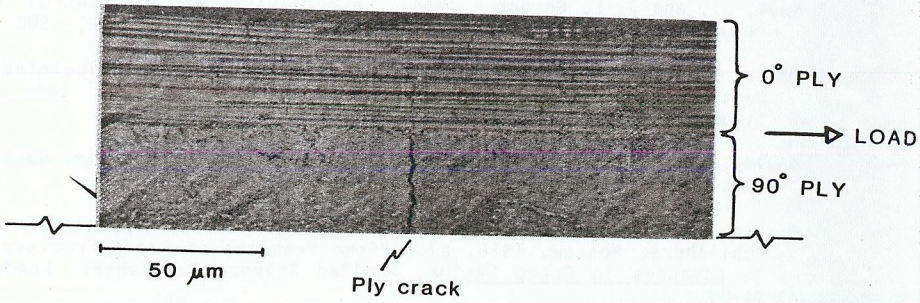

Fig. 1 (a) Characteristic damage state observed shortly prior to the final failure of an epoxy/graphite $[0°, 90°, 45°, -45°]_S$ laminate. The crack seen in the photograph penetrates the 90° ply while the black dots ahead of it represent secondary fractures such as fiber breaks contained within the adjacent 0° ply. Both primary and secondary fractures were made visible by an edge replica technique, cf. Kriz (1982).

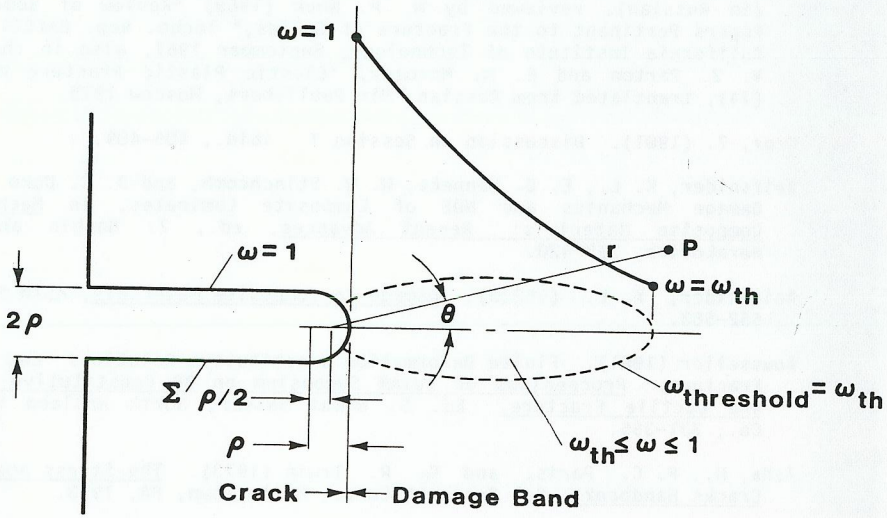

(b) Mathematical model of the physical state depicted in Fig. 1a. The model stems from the continuous damage mechanics (CDM).

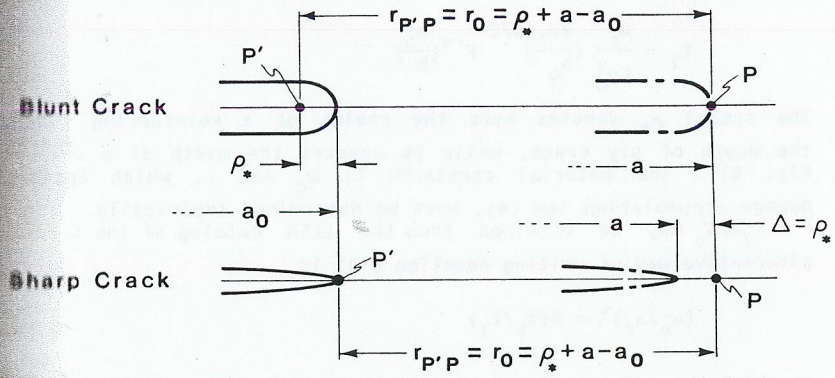

Fig. 2b

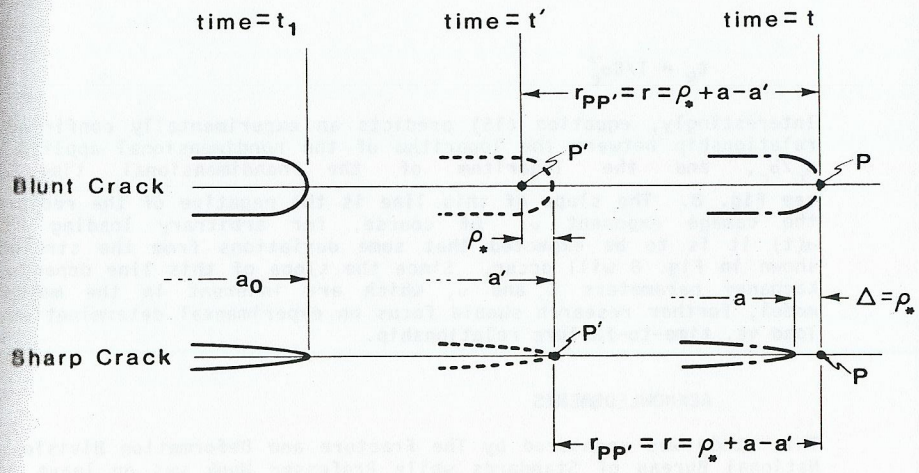

Fig. 2 State of stress $\sigma_\Sigma(P,P')$ generated at the point P while the crack tip is located at the point P' depends on the distance $r_{PP'}$. This distance is shown for (a) stationary crack, and (b) propagating crack. Symbol $\rho*$ denotes the characteristic microstructural length.

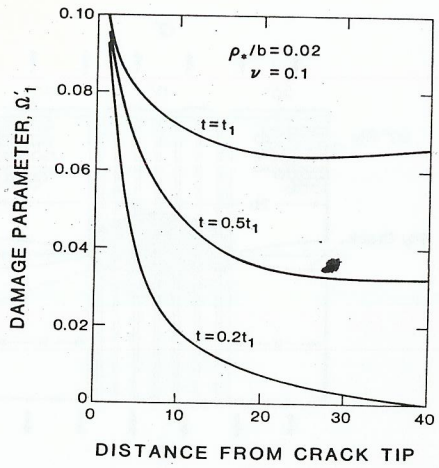

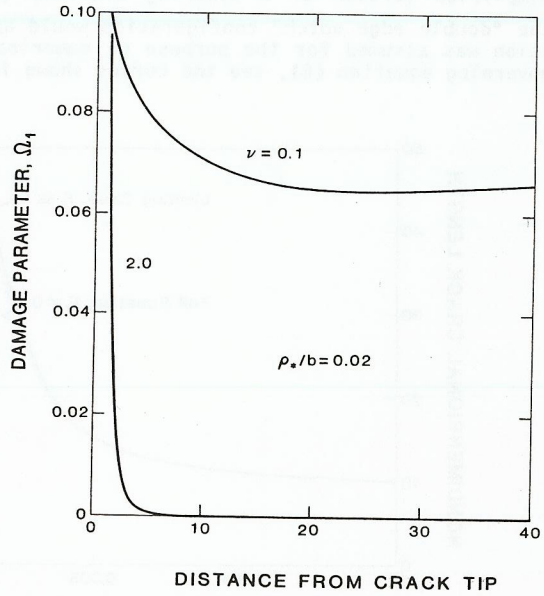

Fig. 3 Distribution of the internal damage (Ω_1) generated during the latent phase of fracture process ($t \leq t_1$) when the dominant crack is stationary. A pronounced difference in the damage accumulation pattern is noted between the two situations, (a) and (b), corresponding to values for the exponent ν of 0.1 and 2, respectively.

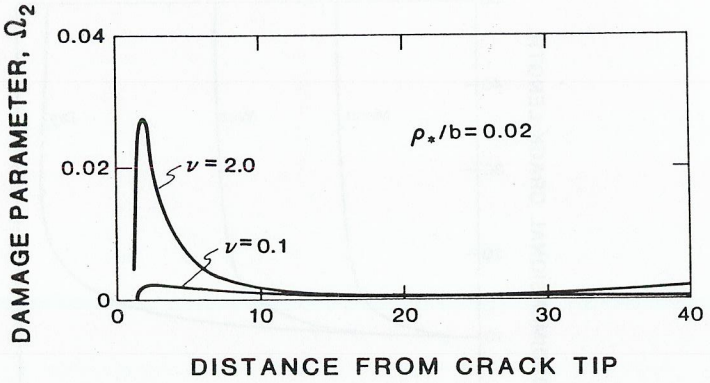

Fig. 4 Distributions of the internal damage (Ω_2) generated during the second phase of fracture process associated with propagation of a dominant crack ($t_1 \leq t \leq t_2$). Two distinctly different situations are obtained for the exponent ν being less than one (ν = .1, Fig. 4a) and greater than one (ν = 2, Fig. 4b).

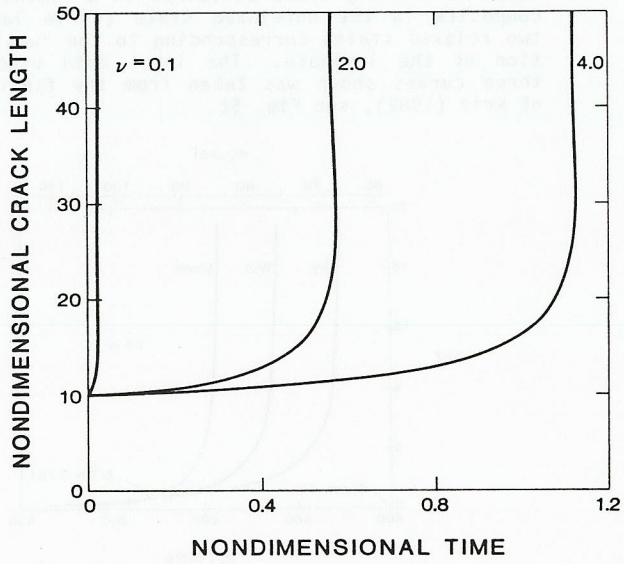

Fig. 5 (a) Second phase of fracture process, i.e., the dominant crack propagation as calculated for ν = .1, ν = 2, and ν = 4 and a stress field σ_Σ generated by a ply crack traversing the remaining ligament that is 0° ply (the crack is shown in Fig. 1). Nondimensional crack length $x = a/\rho*$ is shown as a function of nondimensional time $\theta = t/t_1$.

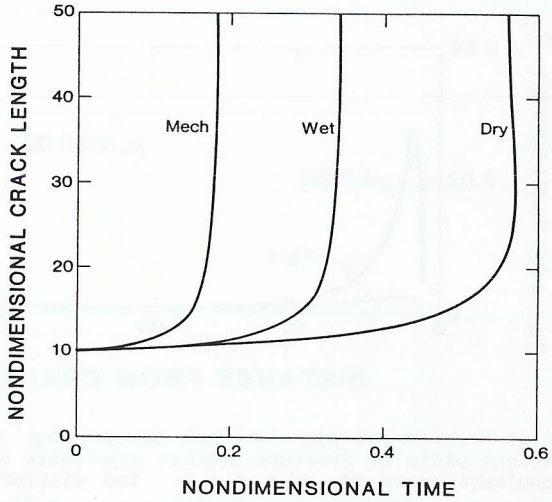

(b) Length of the ply crack vs. time (both nondimensionalized, $\nu = 2$) shown for the three different stress fields generated ahead of the ply crack contained in a laminated epoxy/graphite composite in the unrelaxed state (curve labeled "mech") and two relaxed states corresponding to the "wet" and "dry" condition of the laminate. The input data used to generate the three curves shown was taken from the finite element studies of Kriz (1982), see Fig. 5c.

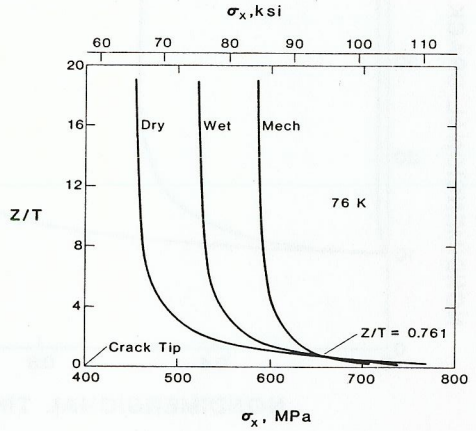

(c) Through-thickness variation of σ_x in 0° ply shown in Fig. 1a for three cases: 1. Mech, mechanical load only with no residual stresses at room temperature, 2. Dry, superposition of residual thermal stresses at 76K in a dehydrated conditions, 3. Wet, superposition of residual stresses caused by swelling when laminate is saturated with absorbed moisture.

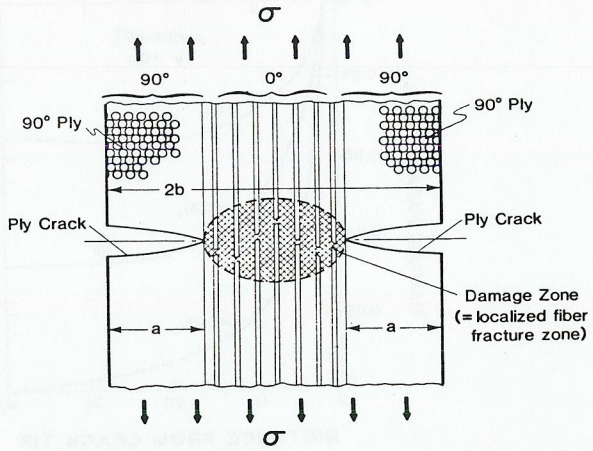

Fig. 6 Simplified version of a stacking sequence $[90°, 0°]_S$ for which the "double edge notch" configuration would apply. This configuration was assumed for the purpose of numerical integration of the governing equation (6), see the curves shown in Figs. 5a and 5b.

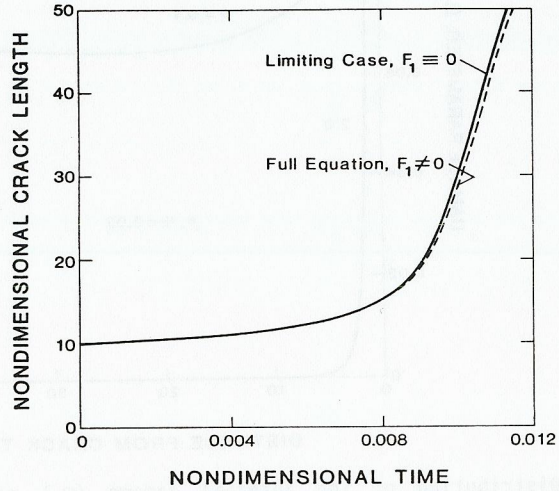

Fig. 7 Comparison between the damage distributions Ω_2, pertaining to the second phase of fracture, as evaluated from the exact (curve 1) and approximate (curve 2) equations. It is seen that for the exponent ν being much less than one ($\nu = .1$) both curves are almost identical.

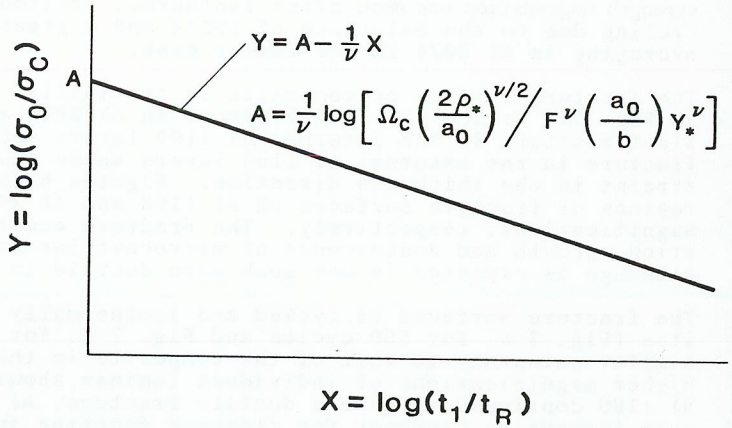

Fig. 8 Straight line shown represents the relation between the constant applied stress σ_0 and the first critical time t_1, see equation (25). Cohesive strength of the reinforcing fiber σ_c is used to normalize stress, while the reference time t_R (= $1/C\sigma_c^{\nu}$) is employed to normalize time.